

Key Properties of Solar Chromospheric Line Formation Process

Zhong-Quan Qu* and Zhi Xu

Yunnan Observatory, Chinese Academy of Sciences, Kunming 650011

National Astronomical Observatories, Chinese Academy of Sciences, Beijing 100012

Received 2001 June 23; accepted 2001 September 13

Abstract The distribution or wavelength-dependence of the formation regions of frequently used solar lines, $H\alpha$, $H\beta$, $CaIIH$ and $CaI18542$, in quiet Sun, faint and bright flares is explored in the unpolarized case. We stress four aspects characterising the property of line formation process: 1) width of line formation core; 2) line formation region; 3) influence of the temperature minimum region; and 4) wavelength ranges within which one can obtain pure chromospheric and photospheric filtergrams. It is shown that the above four aspects depend strongly on the atmospheric physical condition and the lines used. The formation regions of all the wavelength points within a line may be continuously distributed over one depth domain or discretely distributed because of no contribution coming from the temperature minimum region, an important domain in the solar atmosphere that determines the distribution pattern of escape photons. On the other hand, the formation region of one wavelength point may cover only one height range or spread over two domains which are separated again by the temperature minimum region. Different lines may form in different regions in the quiet Sun. However, these line formation regions become closer in solar flaring regions. Finally, though the stratification of line-of-sight velocity can alter the position of the line formation core within the line band and result in the asymmetry of the line formation core about the shifted line center, it can only lead to negligible changes in the line formation region or the line formation core width. All these results can be instructive to solar filtering observations.

Key words: line: formation – radiative transfer – Sun: chromosphere

1 INTRODUCTION

The goal of investigating the line formation theory related to contribution function (CF) lies in the interpreting of the observed data. Unfortunately, such an application was misled to the diagnostics of atmospheric physical parameters without a solid basis established for identifying the line formation depth and the ‘measurement depth’ for a special measurement (Ruiz Cobo

* E-mail: zqqu@cosmos.ynao.ac.cn

et al. 1994; Sanchez Almeida et al. 1990; Qu & Gu 1999). However, this does not mean that the theory has nothing to do with the observations. In fact, it tells us the place where the escape photons originate and thus supplies a useful tool to interpret the filtergrams often used in solar physics. In this paper, we emphasize this application and show what conclusions can be drawn from the exploration and try to give an instruction to the solar filtering observations with frequently used ‘chromospheric lines’.

In our two previous papers (Qu et al. 1999, Paper I; Qu et al. 2001, Paper II; and hereafter), we introduced the concept of ‘*line formation core*’, defined it as one wavelength interval containing the line center, within which all the escape photons come from such regions that are physically identical, and pointed out that this formation region can most suitably represent the line formation region because of the following features.

1) Within the line formation core, the emergent line photons come from the domain which we call the ‘*line formation region*’. It should be noted that this term does not mean that all the wavelength points within the line are formed in this region, it only means the formation region of all the wavelength points in the “line formation core”;

2) The line formation region defined in this way is located in general at the highest atmospheric layers that deviate farthest from the thermodynamic equilibrium (TE), when the magnetic field is absent or has little influence on the line formation process. Only if the line splitting takes place at the line center due to the presence of magnetic field, can the line formation core disappear and does the line-center formation region no longer contains the highest levels (see Paper II);

3) The depth coverage of the line formation region deduced from the above definition is generally more sensitive to the variation of atmospheric thermodynamical condition than the formation regions of the other wavelengths within the line.

4) Neither the width of the line formation core nor its formation region is sensitive to the stratification of the macroscopic line-of-sight velocity, but the formation regions of its neighboring wavelength points are often more influenced by velocity.

In this paper, these features can also be found in the line formation process of four other solar chromospheric lines, than the MgI5172.7 line observed in Paper I.

Generally speaking, four aspects outline the property of line formation process for the solar chromospheric lines. They are: 1) the width of the line formation core; 2) the line formation region; 3) the influence of the temperature minimum region; and 4) the wavelength ranges within which one can obtain pure chromospheric and photospheric filtergrams, respectively. In this paper, we will focus on their dependence on different atmospheric conditions and try to give an answer to issues such as whether one can observe all the layers from the line formation region to the farthest wing formation region using the line-center and off-line-center filtergrams of one line. As will be shown, this issue is tightly linked to the contribution from the temperature minimum region to the emergent line photons.

2 CONTRIBUTION FUNCTION, MODEL ATMOSPHERES AND CALCULATION OF LINE PARAMETERS

According to our previous work (Qu et al. 1999), the emergent intensity can be expressed as

$$I_{\nu}(0) = \sum_{k=1}^n CF_k, \quad (1)$$

where the contribution function to the first-order derivative term of the total source function

with respect to the optical depth reads

$$CF_I(\tau_k) = e^{-\tau_{k-1}} \left[(1 - e^{-\Delta\tau_{k-1}}) S_t(\tau_k) + (1 - e^{-\Delta\tau_{k-1}} - \Delta\tau_{k-1}) \frac{dS_t(\tau_k)}{d\tau} \right], \quad (2)$$

in the above expression k denotes the grid number. The definitions of the other symbols can be found in Paper I.

Equation (1) together with Equation (2) suggest that the contribution from each layer to the emergent intensity originates from a weighted source function and its weighted depth variation along the line of sight. The weighting functions consist of two factors. One is the attenuation factor and the other a modifying one due to the thickness of the layer. For example, the weighting function for the zero-order term is $e^{-\tau_{k-1}}(1 - e^{-\Delta\tau_{k-1}})$. If the thickness $\Delta\tau_{k-1}$ is very small, it tends to $e^{-\tau_{k-1}}\Delta\tau_{k-1}$, and the term containing the factor becomes $e^{-\tau_{k-1}}S_t\Delta\tau_{k-1} \approx e^{-\tau_{k-1}}S_t d\tau$.

Three surface features of solar atmospheres are selected here. They are the average quiet Sun, a faint flare and a bright flare. The average quiet Sun model atmosphere comes from Model C (with 52 grids) of Vernazza et al. (VAL-C,1981) but with a little modification of 47 more grids interpolated and extrapolated by smoothing curves of each parameter. The two flare models originate from Model F1 (with 37 grids) and Model F2 (with 32 grids) of Machado et al. (1980), but also with 62 more grids for Model F1 and 67 more grids for Model F2 interpolated and extrapolated in the same manner. Thus 99 grids in total (with grid number ' $n = 1$ ' representing the uppermost layer and ' $n = 99$ ' the lowest layer of the model atmosphere) are set for each of the three models, and the geometric height ranges are from (-75 km, 2543 km) to (-96.05 km, 2100.03 km) for the average quiet Sun model, and from (100 km, 1459 km) to (-38.12 km, 1461.76 km) for the Model F1 and from (-75 km, 1120 km) to (-69.29 km, 1114.80 km) for Model F2.

Figure 1 illustrates the temperature and electron number density stratification of the three models. Comparing with VAL-C (solid line), F1 (dashed line) and F2 (dotted line) have narrower low temperature regions and low density region under the transition region. In contrast to the temperature enhancement at the top layers of the flare model atmospheres, the electron density drops very rapidly at the transition regions after a lift in the uppermost levels of the chromosphere.

We adopt H α , H β , CaIIH and CaII8542 lines which are frequently used in the diagnostics of the chromospheric structures. These lines are often called '*solar chromospheric lines*'. However, one should remember that this term needs to be more delicately defined, because not all the wavelength points within these lines are formed in the chromosphere, and their line formation regions depend strongly on the thermodynamical conditions. For example, H β , as shown below, formed in quiet Sun is not a pure chromospheric line, because there is a significant contribution from the photosphere to the emergent photons of the line formation core and in the flaring regions, its formation region may contain a part of the transition region.

The calculation code of the line parameters, i.e., damping constant a , Doppler width $\Delta\lambda_D$, line-center and continuum absorption coefficients χ_l and χ_c , as well as line-center and continuum emission coefficients j_l and j_c , is that proposed by Ding and Fang (1989). They considered atomic structures including 12 energy levels plus one continuum state for hydrogen and five levels plus one continuum for once ionized calcium. The relative abundance of CaII is set at 2.14×10^{-6} at each depth grid.

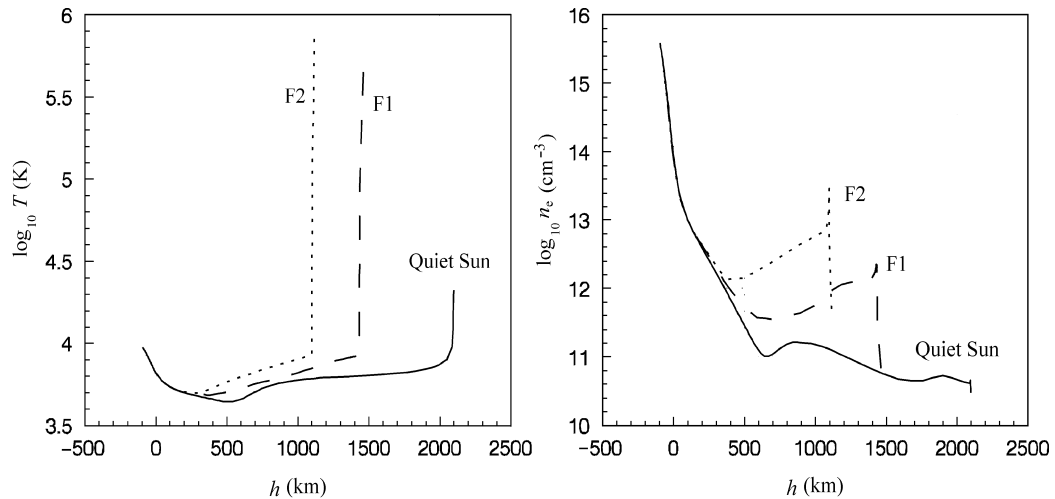


Fig. 1 Sample stratification of temperature and electron number density of model atmospheres. The solid lines indicate those of the model of the quiet Sun (VAL-C), the dashed lines the faint flare (F1) and the dotted the bright flare (F2).

3 FORMATION REGIONS OF $H\alpha$, $H\beta$, CaIIH AND CaII 8542

In the following, the formation properties of $H\alpha$, $H\beta$, CaIIH and CaII 8542 are explored in the quiet Sun, faint flare and bright flare model atmospheres respectively. According to this schedule, the formation properties of different lines in the same model atmosphere are easily compared. However, we will also pay enough attention to the variation of formation regions of each line in the three different atmospheric conditions. We give the detailed information about these four lines in the following Table 1. The influence of line-of-sight velocity is left to the later part of this section.

3.1 Formation Regions in the Quiet Sun

The distributions of formation regions of wavelengths within $H\alpha$, $H\beta$, CaIIH and CaII 8542 can be found in the sample curves in Fig. 2. One of the most striking phenomena is that few escaping $H\alpha$ or $H\beta$ photons are produced in the region (480 km, 600 km) containing the temperature minimum levels, while from this region there are a great amount of CaIIH photons with wavelengths near $|\Delta\lambda| = 280 \text{ m}\text{\AA}$ escaping into space, and a not negligible amount of CaII 8542 photons with wavelengths ranging from $180 \text{ m}\text{\AA}$ to $250 \text{ m}\text{\AA}$. This indicates the difference between the two lines and means that in the quiet Sun, one cannot observe the temperature minimum region via $H\alpha$ and $H\beta$ filtergrams, no matter how wide the bandpass is and where its central wavelength is located. However, it can be seen clearly with filtergrams of CaIIH if the bandpass is placed within the band from $180 \text{ m}\text{\AA}$ to $400 \text{ m}\text{\AA}$. When observing $H\beta$ formation in this surface feature, an unusual phenomenon can be noticed that it is not a pure chromospheric line. Even in the line formation core ($|\Delta\lambda| \leq 40 \text{ m}\text{\AA}$), the photospheric layers just below the temperature minimum region contribute some escape photons (see the solid and dashed lines in the $H\beta$ panel of Fig. 2). This means that the filtering observation using $H\beta$ line cannot

yield pure chromospheric images, though the photospheric ingredient is relatively faint when observing within the line formation core. That also tells us, as an illustration, that it is not suitable to assign a formation depth to a line when the formation region contains two separated domains. This is the reason why we do not generally assign a formation depth to a line.

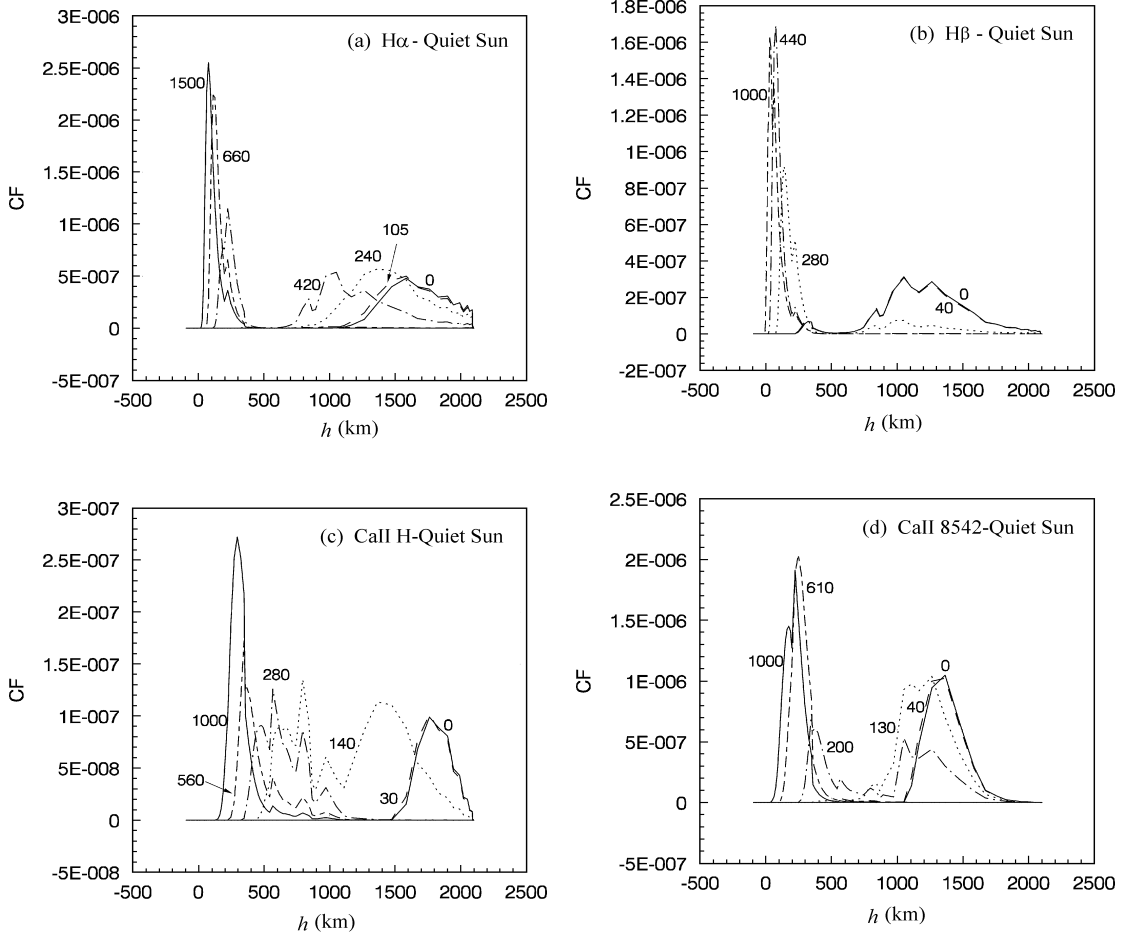


Fig. 2 Formation region distributions of sample wavelength points within the lines H α (a), H β (b), CaIIH (c) and CaII 8542 (d) in the quiet Sun. The labels for each curve indicate the distance from line center in mÅ, and the same are used for the following figures. All the CF's are drawn on the geometric depth scale, the unit is $\text{erg cm}^{-2} \text{s}^{-1} \text{sr}^{-1} \text{Hz}^{-1}$, and hereafter. The greatest number labelling the curve in each panel gives the adopted farthest distance from the line center. Same for the following figures.

3.2 Formation Regions in the Faint Flare

In solar flaring region, the concavity of temperature curve tends to be narrower. Approaching the transition zone, the temperature gradient becomes very great. Meanwhile, the electron density variation turns out to be steeper in the middle and lower layers of the chromosphere and it rapidly decreases in the thin transition region (see Fig. 1). Corresponding to the atmospheric

variation, the lines become emission lines (cf. fig. 26 of VAL and fig. 4 of Machado et al. 1980).

The most striking difference in the line formation regions in the solar flare is that they become very narrow (see all the panels in Fig. 3). For example, the line formation region of $H\alpha$ is markedly compressed from 993 km to 11 km. This signifies that the filtering observation within the line formation core will give an image of very thin layers which can never be acquired in the quiet Sun regions. Comparing with the formation regions of the other wavelength points, the depth coverage of the line formation region is the most sensitive to the variation comparing with other wavelength bands, as we point out in Section 1. The line formation regions of the four lines are closer to each other, a pattern very different from the quiet Sun.

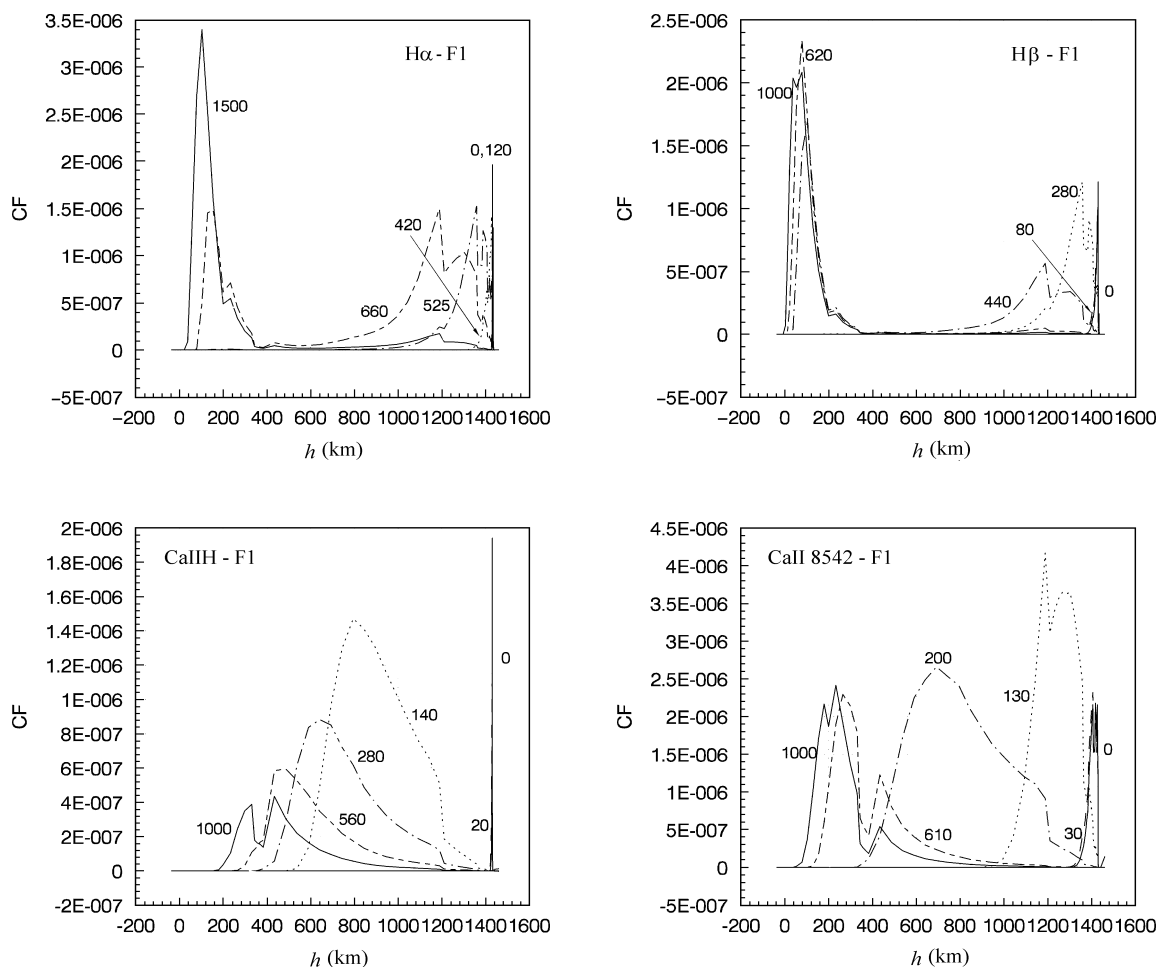


Fig. 3 CF curves of sample wavelength points within $H\alpha$, $H\beta$, $CaIIH$ and $CaII 8542$ lines in the solar faint flare case. It is very marked that the line formation regions of the four lines are much closer to each other than in the quiet Sun. Note that the distribution pattern of formation regions of wavelength points within the two ionized calcium lines is critically changed when compared with the quiet Sun case.

3.3 Formation Regions in the Bright Flare

Few critical changes take place in the bright flaring atmosphere compared with the faint flare case, though much more energy is released in the latter (see Fig. 4). The most outstanding variation occurs in the line formation cores of $H\alpha$, $H\beta$, and $\text{CaII} 8542$ lines which are simultaneously broadened due to their increased Doppler widths. Table 1 shows that their formation core widths are broadened almost by a factor of two in the bright flare than in the faint flare case. The line formation regions of these four lines are further compressed into several kilometers, and their locations as well as depth coverage become further closer to each other. This indicates that the filtering observations with bandpass within the line formation cores of these four lines will give almost the same features of the thin layers of transition region. In the line-center filtering observation, the flare looks like a thin cloud over the background of other surface features. Not only are the line formation regions compressed, but also the formation regions of some other wavelength points. For instance, see $|\Delta\lambda| = 660 \text{ m\AA}$ curve of $H\alpha$, $|\Delta\lambda| = 280 \text{ m\AA}$ curve of $H\beta$, $|\Delta\lambda| = 140 \text{ m\AA}$ curve of $\text{CaII} H$, and $|\Delta\lambda| = 130 \text{ m\AA}$ curve of $\text{CaII} 8542$, and compare with their counterparts in Figure 3.

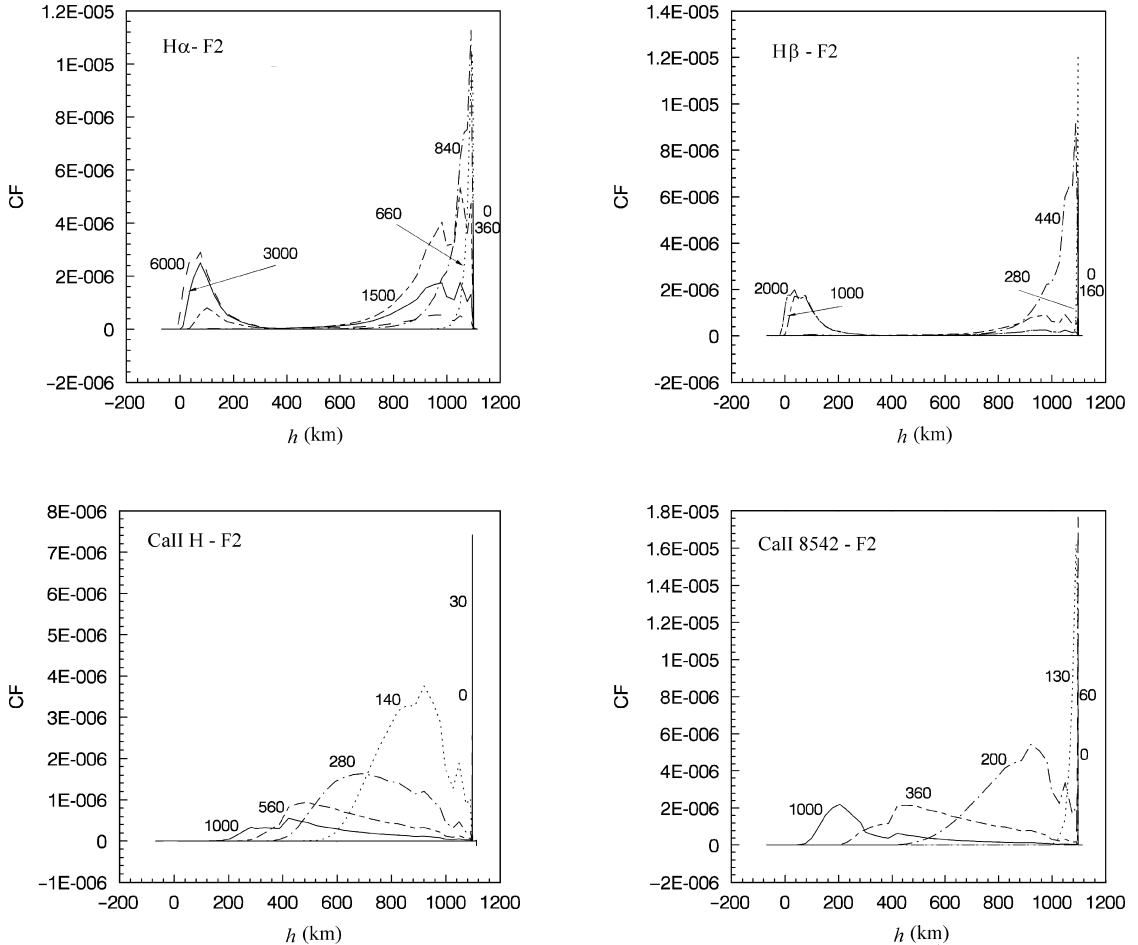


Fig. 4 CF curves of sample wavelength points within $H\alpha$, $H\beta$, $\text{CaII} H$ and $\text{CaII} 8542$ lines forming in bright flare. Note that the line formation regions of the four lines approach each other closer than in the faint case.

3.4 Summary

We discuss in detail the formation properties of the four lines and summarize the above results in Table 1 where the 7 columns list the spectral line, model atmosphere, line formation core width in unit of mÅ, line formation region in unit of 'km', wavelength ranges in unit of mÅ used to obtain the different filtergrams of the temperature minimum region (labelled by Range 1), images of the pure chromosphere (labelled by Range 2) and pictures of the pure photosphere (labelled by Range 3) respectively. In Table 1, 'QS, F1, F2' denote the quiet Sun, faint flare and bright flare, respectively, and 'none' indicates that there is no wavelength points satisfying the observational requirement within the line band adopted. The latter five parameters reflect the most important line formation properties in the sample model atmospheres.

Table 1 Formation Property of H α , H β , CaIIH and CaII 8542 in the Sample Model Atmospheres

Line Used	Model Atmosphere	Formation Core Width (mÅ)	Formation Region (km)	Wavelength Range 1 (mÅ)*	Wavelength Range 2 (mÅ)	Wavelength Range 3 (mÅ)
H α	QS	210	(1107, 2100)	none	$ \Delta\lambda \leq 240$	$ \Delta\lambda \geq 660$
	F1	240	(1426, 1437)	none	525	none
	F2	720	(1097, 1100)	none	900	none
H β	QS	80	(223, 444)(617, 2091)	none	none	380
	F1	160	(1378, 1437)	none	280	none
	F2	320	(1095, 1100)	none	440	none
CaIIH	QS	60	(1473, 2098)	(180, 400)	120	none
	F1	40	(1419, 1433)	(610, 1000)	280	none
	F2	60	(1097, 1100)	(830, 1000)	280	none
CaII8542	QS	80	(1050, 1945)	none	120	450
	F1	60	(1319, 1431)	(280, 580)	220	none
	F2	120	(1090, 1098)	(360, 1000)	220	none

* in this column, the symmetric wavelength interval to the listed in the blue wing also belongs to the range.

It should be pointed out that the values in Table 1 are only deduced from the accepted model atmosphere. They are merely reference values and furthermore only refer to the static atmosphere.

In the above situations, we do not consider the stratification of the macroscopic line-of-sight velocities. In actual situations, it always exists. Therefore one should take it into account. As evidenced in Paper I, though the stratification could change the position of the line formation core of MgI5172.7 and cause the asymmetry of the line core about the shifted line center in the model atmosphere of sunspot umbra, it has little influence on the core width or the line formation region. On the other hand, it does cause changes of the formation regions of some other wavelength points. For instance, at $\Delta\lambda = -150$ mÅ, the concavity covering the temperature minimum between the two major formation regions in fig. 3 (a) of Paper I disappeared in fig. 4 of the same paper.

To investigate the influence on the distribution pattern of formation region of these four lines, we also set some line-of-sight velocity (v_{los}) stratification. In all the cases, the velocity distribution does not alter either the width of the line formation core or its formation region, though its wavelength range is generally shifted with the drift of the line center. The wavelength coverage asymmetry of the line formation core about the shifted line center generally occurs.

Furthermore, the distribution patterns of the formation regions of all the wavelength points within four lines in the three model atmospheres are little affected.

4 DISCUSSION

We have explored the distribution or wavelength-dependence of the formation regions of wavelength points within the frequently used solar chromospheric lines, $H\alpha$, $H\beta$, CaIIH and CaII 8542 in the cases of the quiet Sun, faint and bright flares. We find that the term *solar chromospheric line* should be carefully treated. For even the line formation core, like $H\beta$ in the quiet Sun, the photospheric layers contribute no negligible escape photons, and in the bright flaring regions it can form in the transition region. Though only four lines are studied in this paper, the situation can be applied to other lines. For example, the distribution of formation regions of wavelength points of CaIIH is also suitable for that of CaIIK line, because they have close atomic parameters. The distribution of CaII 8542 can be applied to that of both CaII 8498 and CaII 8662 lines.

It is found that the line formation core is a useful concept in the investigating of line formation property. It is an entity to divide the line band when considering the line formation process. Its wavelength width and formation region are little affected by the stratification of the line-of-sight velocity, and only when the magneto-induced line splitting occurs at the line center does it lose its presence (see Paper II). Furthermore, we have reached the point that if one wants to grasp the property of line formation, the four aspects investigated above should be considered.

We have seen that the formation regions of different lines respond to the variation in atmospheric conditions with different sensitivity. First, the broadening or compressing of the line formation core and line formation region display different sensitivity to the variation when the line formation regions consistently tend to be shallower and narrower in flaring processes. The depth coverage of the line formation region is generally most sensitive to atmospheric physical change. But this does not mean that the formation regions of the other wavelength points within the line do not respond to the variation. Rather! For example, the situation has been met that some wavelength point forms in the photosphere in the quiet Sun but its formation region is located in the chromosphere in the flare case, like $|\Delta\lambda| = 660 \text{ m\AA}$ of $H\alpha$, $|\Delta\lambda| = 440 \text{ m\AA}$ of $H\beta$. Some wavelength point forms in both photosphere and chromosphere in the quiet Sun, like $|\Delta\lambda| = 420 \text{ m\AA}$ of $H\alpha$, but its formation region covers only the chromospheric layers in case of bright flare. More examples can be found, such as the variation in formation region of $|\Delta\lambda| = 280 \text{ m\AA}$ of $H\beta$ from the quiet Sun to the faint flare. Some wavelength points form in the temperature minimum region in the quiet Sun, but its main contribution comes only from the chromosphere in the flares, like $|\Delta\lambda| = 280 \text{ m\AA}$ of CaIIH . Furthermore, even within one line under the same atmospheric variation, the formation region of one wavelength point may be extended while another one may be compressed. On the whole, though the temperature stratification is not the unique ingredient to determine the distribution, it is the most important factor affecting the line formation property. Especially, the temperature minimum region plays a crucial role in these chromospheric line formation processes. According to whether the temperature minimum contributes significantly to the escape line photons, the distributions of formation regions of the wavelength points within the chromospheric lines can be classified into two kinds. One contains a significant contribution from the temperature minimum region and the other does not.

From the account above, the distributions of the formation regions of the two hydrogen lines belong to the first kind and those of the two ionized calcium lines to the second one. However, the v_{los} stratification may change one kind to another, as evidenced in MgI 5172.7 studied in Paper I.

Acknowledgements This paper is sponsored by Item 19973016 of National Science Foundation of China and National Major Project 973 under the grant G2000078401. The authors are grateful to Dr. M. D. Ding for his generous supplying the line parameter calculation.

References

- Ding M. D., Fang C., 1989, *A&A*, 225, 204
Machado M. E., Avrett E. H., Vernazza J. E., Noyes R. W., 1980, *ApJ*, 242, 336
Qu Z. Q., Zhang X. Y., Gu X. M., 1999, *MNRAS*, 305, 737 (Paper I)
Qu Z. Q., Zhang X. Y., Xu Z., 2001, *Chin. J. Astron. Astrophys.*, 1(2), 161 (Paper II)
Qu Z. Q., Gu X. M., 1999, In: Nagendra & Stenflo, ed., *Solar Polarization*, Kluwer Academic Publishers, p.291
Ruiz Cobo B., del Toro Iniesta J. C., 1994, *A&A*, 283, 129
Sanchez Almedia J. et al, 1996, *A&A*, 314, 295
Vernazza J. E., Avrett E. H., Loeser R., 1981, *ApJS*, 45, 635